Separation Science and Technology
Publication details, including instructions for authors and subscription information:
http://www.informaworld.com/smpp/title~content=t713708471

Removal of As(V) Using an Iron-Impregnated Ion Exchange Bead

Laura E. LeMire[a]; Miguel A. Teixeira[b]; Brian E. Reed[a]
[a] University of Maryland, Baltimore County, TRC Building, Baltimore, MD, USA [b] Faculdade de Engenharia da Universidade do Porto, Portugal, Porto, Portugal

Online publication date: 15 September 2010

To cite this Article LeMire, Laura E. , Teixeira, Miguel A. and Reed, Brian E.(2010) 'Removal of As(V) Using an Iron-Impregnated Ion Exchange Bead', Separation Science and Technology, 45: 14, 2051 — 2063
To link to this Article: DOI: 10.1080/01496395.2010.504433
URL: http://dx.doi.org/10.1080/01496395.2010.504433

Separation Science and Technology, 45: 2051–2063, 2010

ISSN: 0149-6395 print/1520-5754 online
DOI: 10.1080/01496395.2010.504433

Taylor & Francis
Taylor & Francis Group

Removal of As(V) Using an Iron-Impregnated Ion Exchange Bead

Laura E. LeMire,[1] Miguel A. Teixeira,[2] and Brian E. Reed[1]
[1]*University of Maryland, Baltimore County, TRC Building, Baltimore, MD, USA*
[2]*Faculdade de Engenharia da Universidade do Porto, Portugal, Porto, Portugal*

The ability of an iron-impregnated ion exchange bead (PWX5) to remove As(V) from ground water was investigated. The effects of particle size, solution pH, As(V) concentration, competition, adsorbent concentration, temperature, iron content, and iron accessibility on removal kinetics and/or equilibrium were determined. PWX5's performance was compared to other iron-based adsorbents, primarily Bayoxide® E-33 (E-33), a granular ferric oxide, for arsenic removal performance. All of the factors cited impacted either the amount of As(V) adsorbed or the rate of adsorption. Stirred batch reactor data showed the rate of adsorption increased as particle size decreased and bottle point isotherm data showed As(V) adsorption maximum capacity increased with higher initial adsorbate concentration. The presence of phosphate and silicate reduced the amount of As(V) adsorbed as did a pH > 7.0. PWX5 is durable, rather homogeneous in size and effective at removing As(V). It is a viable alternative to E-33 which has a wider size distribution and wears more easily.

Keywords adsorption; anion ligand exchange; arsenic removal; drinking water; granular ferric oxide; iron impregnation; particle size

INTRODUCTION

Arsenic contaminated groundwater is an environmental problem impacting millions of people across the globe. Although the concentration of arsenic found in natural waters is typically less than 10 μg/L, it can be in excess of 5000 μg/L (1). In 1998, to protect human health, the European Union issued a Directive decreasing the allowed concentration from 50 μg/L to 10 μg/L, effective November 23, 2000 (2). In 2001, the U.S. Environmental Protection Agency (USEPA) reduced the maximum contaminant level from 50 to 10 μg/L as well, with an effective compliance date of January 23, 2006, impacting more than 13 million people at a national cost of compliance of approximately $120 million per year in 1999 dollars (3).

A range of materials and processes have been studied for the removal of arsenic from contaminated drinking water. Conventional methods which utilize lime, alum, or ferric sulfate as a coagulant, produce a wet bulky precipitate that requires secondary treatment (4). Coagulation processes are expensive and not appropriate for small treatment facilities (5). Currently, the most cost effective and commonly used methods are co-precipitation and adsorption on iron oxyhydroxides (6) and activated alumina in a fixed-bed system (5,7). Although ion exchange, activated alumina, reverse osmosis, and modified coagulation/filtration were specified by USEPA as the most effective best available technology (8), adsorption systems offer the most promise for arsenic removal in small systems based on cost and space requirements (9). In addition to iron, hydroxides of aluminum also strongly adsorb or form an insoluble precipitate with arsenites and arsenates, which exhibit typical sorption behavior of anions in the form of oxyanions (9,10).

For adsorption processes, granular ferric oxides and hydroxides or activated alumina (AA) in a fixed bed system are the preferred adsorbents as a result of their removal efficiency and availability, and the similarity of their operation requirements to those of activated carbon beds. Selvin et al. reported that of more than 50 media tested in the lab for arsenic removal, GFH®, a commercially available, granular ferric hydroxide, was the most effective (5,11) and GFH experiments by Amy et al. indicate it may have five times the capacity of AA (12). Of those adsorbents tested by Sandia National Laboratories, Bayer AG Bayoxide® E 33 (E-33), a commercially available granular ferric oxyhyroxide was the most effective (13). Westerhoff et al. reported that at five Arizona well sites, E-33 and GFH performed similarly; however, at one site, E-33 provided 50% more treatability for arsenic than GFH (14). However, GFH (a poorly crystallized β-FeOOH (7)) and E-33 (a synthetic iron oxide hydroxide, α-FeOOH) wear easily; a detriment to plant operations as the head loss increases as the material physically breaks down requiring the adsorbent to be backwashed.

Given that iron oxide is an accepted adsorbent for As(V), identifying a more durable and efficient Fe-based adsorbent would be beneficial. Polymer ligand exchangers, composed of a cross-linked hosting resin that is firmly

Received 13 March 2009; accepted 3 June 2010.
Address correspondence to Laura E. LeMire, University of Maryland, Baltimore County, TRC Building, Baltimore, MD 21227, USA. Tel.: (443)-840-5904; Fax: (443)-840-4744. E-mail: llemire@ccbcmd.edu

bound with Fe^{3+}, are a viable alternative. Because these resins use metal ions for the terminal functional group, the ligand exchange involves concurrent Lewis acid-base interactions as well as electrostatic interactions (15). PWX, an iron impregnated ion exchange bead, removes As(V) via the same mechanism as GFH and E-33 (ligand exchange with the hydroxyl group), is more durable, and has potentially higher As(V) capacity and faster kinetics due to a more uniform and accessible Fe-oxide phase.

The objectives of this study were to determine the PWX As(V) isotherm and kinetic behavior as a function of particle size, solution pH, As(V) concentration, the presence of other oxyanions (SiO_2, PO_4^{3-}), adsorbent concentration, temperature and iron content, and to compare the performance of PWX with that of commercial grade GFH and E-33.

EXPERIMENTAL DESIGN

Materials

PWX (a weak base resin) and iron impregnated PWX were supplied by Rohm and Haas (Philadelphia, Pennsylvania). Due to proprietary reasons, the details of the iron impregnation procedure and polymer composition cannot be described. During the course of development, five versions of PWX were manufactured (identified sequentially as PWX1, PWX2, PWX3, PWX4, and PWX5). E-33 was supplied by Bayer (Monheim am Rheim, Germany). For most experiments, the synthetic water recommended by the National Sanitation Federation (NSF), Standard 53 Challenge Water, was used (see Table 1). Unless otherwise specified, the pH was adjusted to 6.5 using hydrochloric acid (HCl). As(V) used to spike the challenge water was prepared using Sigma-Aldrich disodium hydrogen arsenate heptahydrate (Na_2HAsO_4-$7H_2O$), ACS Reagent.

EXPERIMENTAL APPROACH

The adsorbents were first characterized by particle size distribution, iron content (by particle size), acid-base behavior, and physical shape. The effect of drying and grinding the materials was then determined. Adsorption pH-edges were designed to determine the effect of pH, iron content, adsorbent concentration, and competing adsorbates (phosphate and silicate) on As(V) removal. The effects of sulfate and calcium were not evaluated, as prior researchers working with hydrous ferric oxide, ferric chloride, bauxol, and GFH reported little or no adverse impact on As(V) removal and even a beneficial effect in some cases with calcium present (5,9,10,16,17). Isotherms were conducted as a function of particle size at multiple adsorbate concentrations and as a function of temperature. Batch kinetic tests were conducted to determine the effect of size and adsorbent concentration on the rate of arsenic adsorption.

TABLE 1
Challenge water parameters

Parameter	Target concentration	
As(V)	100 μg/L	1.33×10^{-6} M
Mg^{+2}	12 mg/L	494×10^{-6} M
NO_3^-	2 mg/L	32.3×10^{-6} M
SiO_2	20 mg/L	333×10^{-6} M
PO_4^{-3}	40 μg/L	0.42×10^{-6} M
$NaHCO_3$	250 mg/L	2.98×10^{-3} M
Ca^{+2}	40 mg/L	998×10^{-6} M

METHODS

Particle Size Distribution

The adsorbents were wet-sieved with deionized (DI) water through a series of ASTM standard sieves: U.S. mesh no. 16 (1180 μm), 18 (1000 μm), 30 (600 μm), 40 (425 μm), and 60 (250 μm). The contents retained on each sieve were placed into containers and re-sieved starting with the sieve on which they were retained. The sieved material was collected again and sieved a third time in the same manner. The PWX5 was stored in DI water to prevent shrinkage. The E-33 material was sieved carefully to avoid altering the as-received (not sieved) sizes of the soft particles which disintegrated easily.

Iron Content

A known amount of PWX5 was added to a 50 mL vial containing 45 mL of 10% sulfuric acid (H_2SO_4) solution and shaken for four days. The contents of the vial were allowed to settle for two hours, after which time 40 mL of solution was removed, tested for iron content, and retained in a separate plastic container. The vial was refilled with 40 mL of fresh acid solution and the process was repeated until the concentration of Fe in the diluted solution was below the detection limit of 1 mg/L. For E-33, the vials were shaken for two days and then filtered through a 45 μm filter. The filter was placed in the vial with the E-33 which was refilled with 45 mL of sulfuric acid. The process was repeated until the iron concentration was no longer detectable in the filtrate.

Acid/Base Behavior

Titrations were conducted on virgin PWX (i.e., no iron), impregnated PWX5, and E-33 over a pH range of 3.5 to 11 using a Tanager Scientific Systems Inc., dual pH meter and a titrator (Model 8901). The adsorbent solution concentration was 10 mg/L and the ionic strengths tested were 0.001 M and 0.01 M (as $NaNO_3$). For each ionic strength, four 40 mL samples were prepared. One sample was titrated with 0.1 N NaOH and one with 0.1 N HNO_3. The automatic titrator delivered the titrant such that the maximum change in pH was less than 0.15 pH units. The dosing rate

was calculated automatically by the titrator and was not constant. The remaining two samples were filtered using 0.45 μm filters and the filtrate was titrated with either the acid or the base. The curves for the acid and base legs were combined for both the filtrate and the suspension. The filtrate curve was then subtracted from the suspension curve to generate a net titration curve that represents the acid-base behavior of the surface.

Effect of Drying and Grinding

Drying and grinding the adsorbent for use in isotherms and pH-adsorption edges is a standard approach for most adsorbent materials. Adsorbents are generally dried to accurately determine the mass being utilized and ground to reduce the time to reach equilibrium. For activated carbons, it is accepted that grinding the material does not increase the removal capacity; however, the effect of drying and/or grinding for E-33 and PWX5 are not as well known and need to be determined, as removal capacities are used in the design of full-scale systems. Stirred batch reactor tests were run on E-33 and PWX3 for a period of seven days with samples taken at 1, 3, and 7 days. In each test, 0.033 g/L (dry weight) of adsorbent was added to a solution containing 1160 μg/L of As(V) and 100 mg/L of $NaHCO_3$ at a pH of 8.0. PWX3 was tested as-received with the following starting physical conditions:

1) wet (original moisture content of about 53%),
2) dried at 101°C, and
3) dried at 101°C and coarsely ground to pass the No. 140 sieve (106 μm).

In addition, two finely ground samples of PWX3 were tested. One sample passed the No. 100 sieve (150 μm) and was retained on the No. 200 sieve (75 μm), and the other passed the No. 200 sieve. E-33 was tested with the same starting physical conditions (original moisture content of 43%), but was sieved prior to testing ($35 \times 40 - 500\ \mu m \times 425\ \mu m$).

Effect of pH on As(V) Removal

To determine the effect of pH on As(V) adsorption, pH-adsorption edges were run on PWX5, E-33, and virgin PWX beads. Each material was dried and ground to pass a No. 200 sieve. Solutions of 10 mg/L, 20 mg/L, and 40 mg/L of PWX5, 10 mg/L of E-33 and 30 mg/L of virgin PWX in DI water containing 100 μg/L As(V) were prepared. While rapidly stirring, twelve 50 mL vials containing eight glass beads were filled with 53 mL of the adsorbent slurry. Head space in the vials was minimized to avoid interaction with the atmospheric CO_2. The pH of each vial was adjusted to obtain pH values ranging from 3 to 12 using 0.1 N HC1 or 0.1 N NaOH. After the vials tumbled for four days in a rotary agitator, the pH of the suspension was measured and the samples were filtered through a 0.45 μm cellulose filter, acidified, and analyzed for arsenic.

Adsorption Isotherms

Isotherms were conducted at 21°C using ground PWX and E-33 at adsorbent concentrations ranging from 0.73 to 40 mg/L. The adsorbents were added volumetrically from a rapidly mixing 1 g/L slurry. Pipette tips were cut to allow the suspended adsorbent particles to freely enter the pipette. The adsorbent was pipetted into 50 mL vials containing glass beads for mixing. The vials were filled with NSF challenge water and tumbled for six days. The six day equilibration period was used as a result of O'Connor's determination that rapid attainment of equilibrium may be inappropriate for multi-adsorbate systems (18). The pH of each suspension was then measured and the samples filtered through a 0.45 μm filter and acidified to a pH of 2.

To determine the effect of temperature, isotherms were repeated at 1°C and 36°C using 50 mL of challenge water per vial and a three day mixing period. The 1°C and 36°C samples were placed in a covered shaker instead of a tumbler to maintain temperature. The duration of the isotherm tests was reduced to three days based on the batch kinetic experiments.

As(V) Removal Kinetics

Batch kinetic tests were conducted using four size fractions of PWX5 (ASTM sieves: 16×18, 18×30, 30×40, and 40×60) as well as four concentrations of as-received PWX5 (8.0, 15.3, 20.0, and 30.1 mg/L). Two liter volumes of NSF challenge water were placed on stirrers and the speed adjusted till the vortex of each solution was of equal depth. The surface of the solution was covered with a plastic film to minimize interaction with the atmospheric CO_2, which allowed for better pH control. Prior to each sample extraction, the stirrers were turned off briefly to allow the particles to settle. Samples were taken using a 1–5 mL pipette positioned 1–2 cm below the surface. A total of twenty 5 mL samples were taken throughout the experiment. E-33 was not tested because the material physically degraded while mixing, altering the particle size and, as will be discussed later, the As(V) removal capacity.

ANALYTICAL METHODS

Arsenic concentrations were determined using the Perkin-Elmer Graphite Furnace Atomic Absorption Spectrometer 4100ZL (GFAA). Arsenic standards were prepared using 1,000 ppm Fisher Scientific Arsenic Reference Solution, with arsenic trioxide (As_2O_3) as the solute. Iron concentrations were determined using a Perkin-Elmer flame atomic absorption spectrophotometer. Standards were prepared using Acros Iron atomic absorption standard solution, 1 mg/mL Fe in 0.2% HNO_3.

RESULTS AND DISCUSSION

Particle Size Distribution

Particle size results (see Fig. l) show that PWX5 and E-33 have mean diameters of 670 μm and 728 μm respectively. PWX5 is more homogeneous with approximately ninety percent of the beads having diameters between 425 and 1000 μm. The heterogeneous sizing of E-33 results in lower porosity in a fixed-bed system and contributes to the need for backwashing which is typical in most filtration systems (19). The amount of E-33 smaller than the No. 35 sieve (0.5 mm) was found to be around 30%, exceeding the maximum 20% specified on the manufacturer's Technical Data Sheet. Despite the careful handling of the material, some of the discrepancy can be explained by the breakdown of larger particles during testing due to the friability of E-33. The mean diameter for E-33 is larger than the 500–650 μm average particle size range for GFH reported by Saha et al. (7). Optical microscope photographs of PWX4 and E-33 are included as Fig. 2. PWX is spherical in shape and smooth while E-33 is angular and jagged.

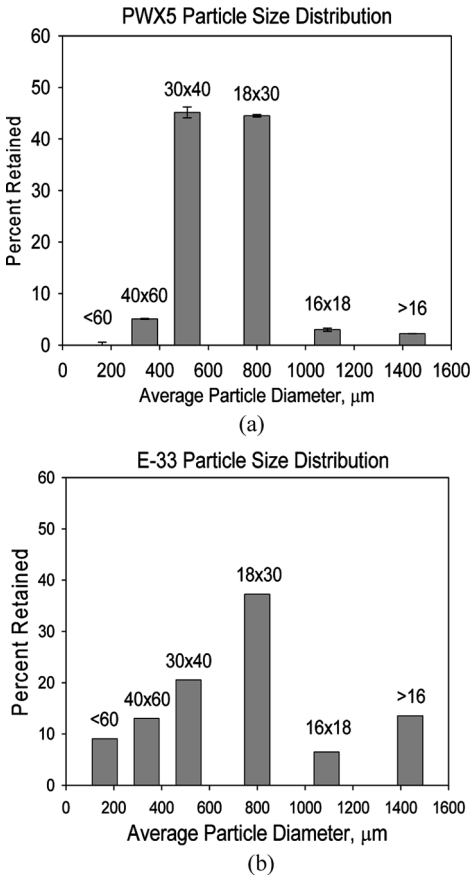

FIG. 1. PWX5 and E-33 particle size distribution by average particle diameter. Average diameter is defined as the average of the two sieve sizes for the range.

Iron Content

During the development of the PWX material, the iron content was increased progressively (see Table 2) to maximize the amount of iron deposited throughout the particle while minimizing the reduction in internal access (as iron oxide content increases, it is possible to block access to the interior of the bead). All As(V) removal experiments relevant to water treatment were conducted on PWX5, the final version.

Iron content as a function of particle size is presented in Fig. 3. For PWX5, the iron content increased slightly with particle size possibly due to the larger particles having larger pore diameters which allowed the iron to penetrate deeper into the bead. The predominant size particles, 18×30 and 30×40, contained 16.8% and 16.3% iron respectively which were in agreement with the PWX5 as-received iron content of 16.0%. For E-33 16×18, as-received, and 40×60 size particles, the iron content is close to 63%, which corresponds to the percentage of iron found in goethite, FeOOH (62.9% by molecular weight).

Effect of Grinding and Drying

PWX grinding required extensive effort while E-33 was easily ground making it clearly apparent that PWX is much more durable than E-33. Grinding and drying the adsorbent did not have a significant effect on PWX performance, as shown in Fig. 4. Equilibration was reached after approximately 3 days, after which time the As(V) concentration increased slightly over the remainder of the 7 day period possibly due to changes in pH (pH increased slightly) or the slower adsorption rate of competing ions (with time, As(V) was displaced by other anions). Drying had little effect on E-33 performance, but grinding the material increased As(V) removal resulting in E-33 outperforming PWX on an adsorbent mass basis. It is hypothesized that grinding increased the number of FeOH sites available for ligand exchange. The E-33 results are in agreement with research conducted by Yean et al. who demonstrated that the adsorption capacity for arsenic by lab prepared magnetite completely dispersed in solution was significantly greater than commercially prepared magnetite, and determined that it may be a result of more adsorption sites being exposed to the arsenic (20). Based on the results shown in Fig. 4, it appears that data generated from the isotherm, the pH-adsorption edges, and other experiments conducted using ground E-33 overestimates the As(V) removal capacity. Finally, the similarity of As(V) removal behavior of PWX3 beads and of ground PWX3 indirectly indicates that most of the impregnated iron oxide is accessible. This conclusion is supported by the comparison of As(V) removal on a Fe basis with PWX3 performing better than E-33, possibly due to the iron oxide being more evenly distributed on the bead surface exposing more sites than

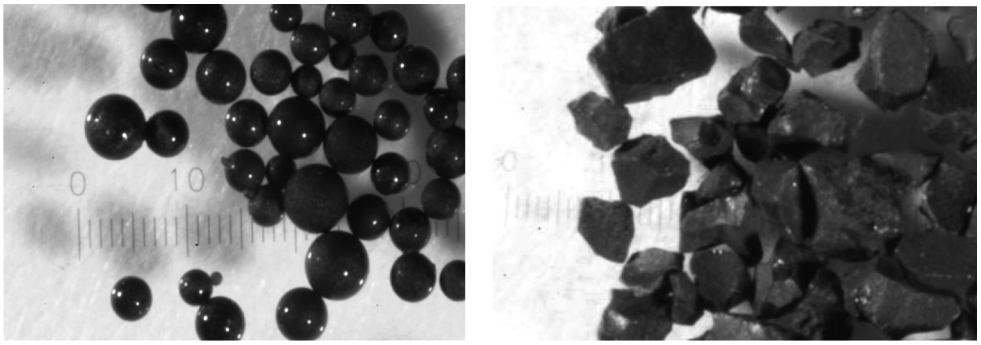

FIG. 2. Optical microscope photograph of PWX4 (left) and E-33 (right), 1 unit = 100 μm.

available on even ground E-33, unless the iron oxides are fundamentally different with the PWX iron oxide having inherently more sites per gram.

Acid/Base Behavior

Titration results for impregnated PWX5 and virgin beads are presented in Fig. 5. The pH of the virgin PWX samples ($I_{.01}$ = pH 9.8, $I_{.001}$ = pH 9.5) was higher than PWX5 ($I_{.01}$ = pH 5.9 and $I_{.001}$ = pH 7.0) due to the basic nature of the as-received PWX bead and the acidic nature of the impregnated iron. The pH_{zpc} (the pH at which the positive and negative charged surface sites are equal, net surface charge is zero) for iron oxides ranges from 6.5 to 9 depending on the mode of formation and age of precipitate (21). The pH_{zpc} of E-33 is ~8.5–8.6 which falls in the range of the pH_{zpc} of goethite (7.5–9.2). pH_{zpc} for GFH is slightly lower at ~8 (14,22). For most adsorbents, the pH_{zpc} can be determined from the intersection of the acid-base titration curves at low ionic strengths; however, this method is suspect with the PWX adsorbents because the non-iron oxide sites on the resin material can uptake OH^- (when the base is added) and NO_3^- (when titrated with an HNO_3). Thus, when discussing the pH dependent behavior of As(V) removal by PWX5, it will be assumed that the iron oxide portion of the adsorbent is amphoteric with a pH_{zpc} of about 7.5. The weak base resin sites are not amphoteric and do not contribute to the pH dependent behavior of As(V) removal (the later observation is supported by the virgin PWX pH adsorption edge results which show that As(V) removal by virgin PWX is not a function of pH).

TABLE 2
PWX iron content during product development

Version	Iron Content, %
PWX1	2.4–3.5
PWX2	9.7–13.5
PWX3	9.2–10.1
PWX4	13.0–13.7
PWX5	15.8–16.1

Effect of pH and Competition with SiO_2 and PO_4^{3-}

As(V) removal was a function of pH for both E-33 and PWX5 but not for virgin PWX. At an adsorbent concentration of 10 mg/L, arsenic removal was highest below

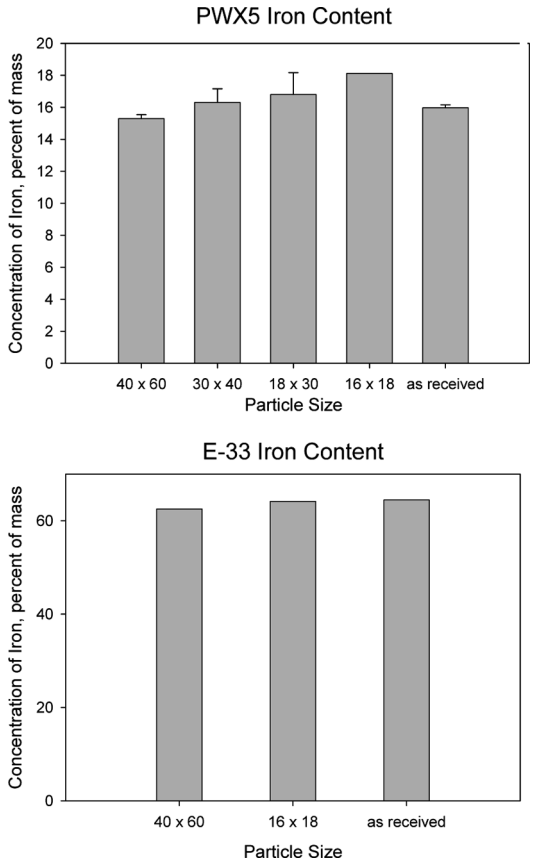

FIG. 3. Iron content of PWX5 and E-33 by particle size.

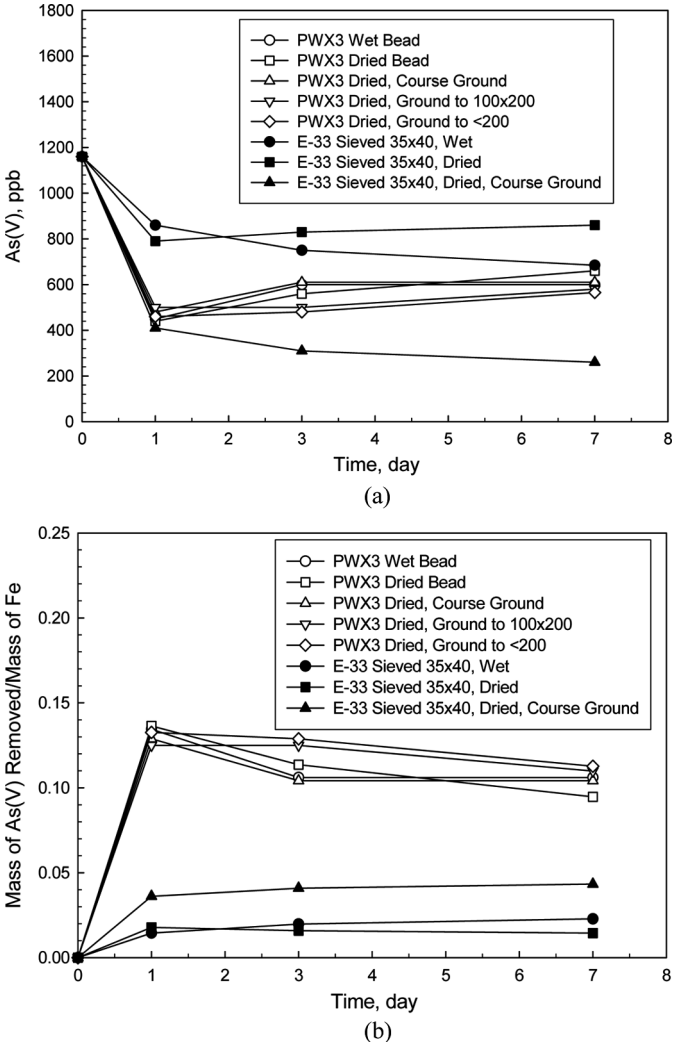

FIG. 4. Effect of grinding and drying on As(V) adsorption presented as: a. As(V) concentration in solution, and b. As(V) removal in relation to the iron content of the media. All tests used a dry adsorbent concentration of 0.033 g/L, As(V) 1160 ppb,$NaHC0_3$ 100 ppm and pH 8.0.

pH 7.0 and decreased sharply between pH 7.0 and 8.5 as illustrated in Fig. 6. At a concentration of 30 mg/L, the edge for PWX5 shifted to the right (higher removal) with arsenic removal declining sharply between pH 8.0 and 10.0 as a result of more high energy sites being available at the higher adsorbent concentrations. Reed and Vaughn found that a similar shift occurred as the concentration of iron impregnated activated carbon increased (23). Increasing the concentration of PWX5 three-fold resulted in an increase in arsenic removal of about 37%. At 30 mg/L, the virgin PWX exhibited consistent arsenic removal of approximately 17%, which is significantly lower than the iron impregnated bead.

The amount of arsenic removed is a function of iron content as well as pH. E-33, with about four times the iron

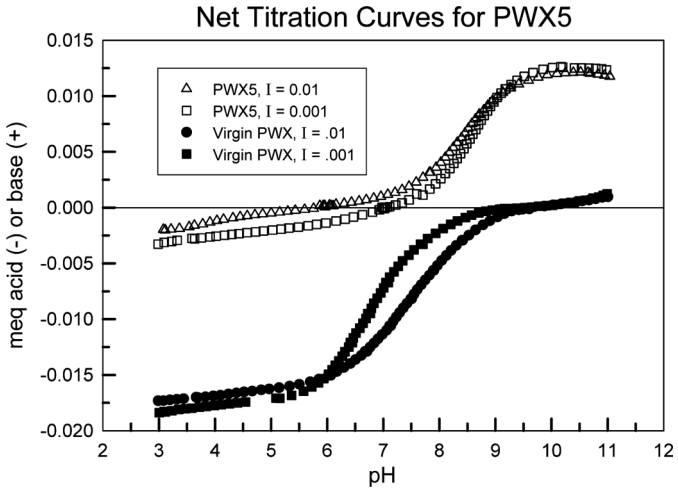

FIG. 5. Net titration curves for PWX5 and virgin PWX at various ionic strengths.

content of PWX5 (6.3 mg/L vs. 1.6 mg/L), removed about 25% more arsenic than PWX5 at the same bulk adsorbent concentration (10 mg/L). Likewise, PWX5 at an adsorbent concentration of 30 mg/L, containing three times the amount of iron as 10 mg/L of PWX5, removed roughly 38% more arsenic.

By plotting the pH-adsorption edges based on the amount of As(V) removed per mole of iron in the adsorbent (see Fig. 7), it can be determined that accessibility of the iron oxide surface sites had a significant impact on the amount of As(V) removed. At 10 mg/L, PWX5 containing 1/4 as much iron as E-33 removed nearly three times more As(V) per mole of iron (26×10^{-3} mol As/mol Fe compared with 9×10^{-3} mol As/mol Fe). At 30 mg/L, PWX5 containing 24% less iron than 10 mg/L of E-33, removed roughly 8% more As(V) on a mass basis and 28% more

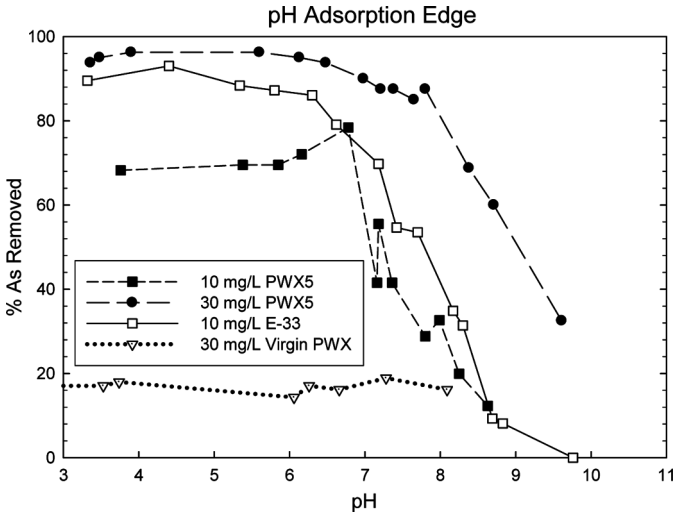

FIG. 6. pH adsorption edges for PWX5, E-33 and virgin PWX.

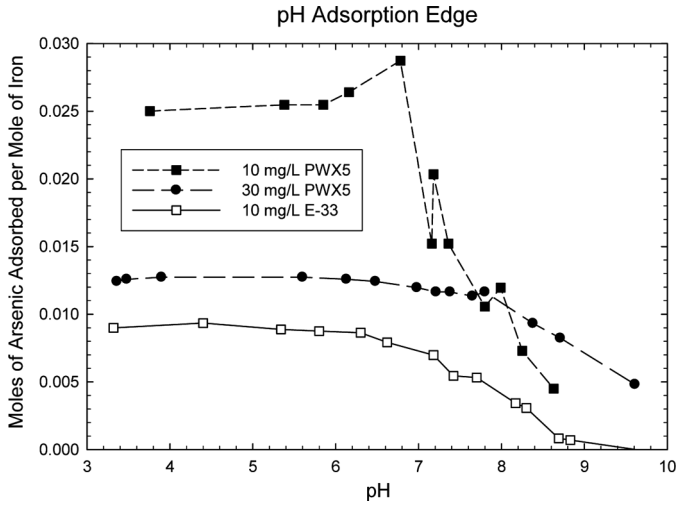

FIG. 7. pH adsorption edges showing arsenic removal in relation to the iron content of the media.

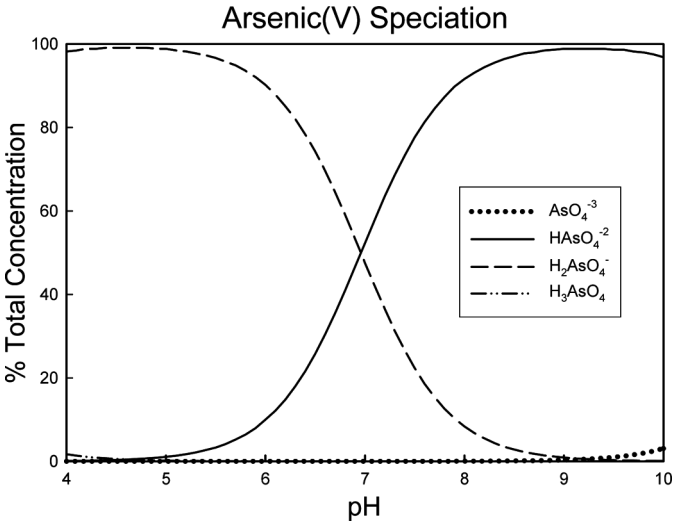

FIG. 8. Speciation diagram for As(V).

on a mole basis. The difference in As(V) removal by the two adsorbents increased with increasing pH. In addition, PWX5 at a concentration of 10 mg/L, removed twice as much As(V) per mole of iron as PWX5 at 30 mg/L (12.5×10^{-3} mol As/mol Fe).

These results indicate that the iron in E-33 is not fully accessible, contains fewer adsorbent sites, and/or contains weaker sites than PWX5. The iron in PWX5 essentially coats the external surface and pore walls, whereas the iron in E-33 is imbedded throughout the material and is not readily accessible to As(V) in solution. The result is greater arsenic removal by PWX5 at a lower iron concentration. Also, at lower concentrations of PWX5, the amount of As(V) in solution after strong OH exchange sites have been bound is greater than in a slurry with 30 mg/L of PWX5, resulting in a stronger driving force for the As(V) to exchange with weaker sites.

The effect of the solution pH on adsorption of As(V) onto PWX5 and E-33 is consistent with the behavior observed for As(V) and other iron oxide adsorbents (5,23–25). The speciation diagram for As(V) is presented in Fig. 8 using MINEQL. Since adsorption occurs via a ligand exchange with OH^-, when the concentration of hydroxide increases in the aqueous phase, the driving force for the exchanged hydroxide to move to the bulk aqueous phase decreases (26). Also, as the pH approaches the pH_{zpc}, the surface of the adsorbent becomes less positively charged, reducing electrostatic attraction. At $pH > pH_{zpc}$, both the surface and As(V) are negatively charged resulting in electrostatic repulsion which contributes to a decrease in removal.

The effect of competition on As(V) adsorption is presented in Fig. 9. Tests were run with silicate (SiO_2) and phosphate (PO_4^{3-}) ratios similar to the challenge water ratios of 1:250 As:SiO_2 and 1:0.31 As:PO_4^{3-}. The presence of SiO_2 and PO_4^{3-} reduced the amount of arsenic adsorbed compared to arsenic alone, with SiO_2 having the greatest impact.

The addition of PO_4^{3-} at a 1:1 As:PO_4^{3-} molar ratio reduced the percent of arsenic adsorbed by 10% to 20% between pH 7.0 and pH 10.0. Although the concentration of phosphate in the challenge water is lower than that of arsenic, it often exceeds a 1:1 molar ratio in groundwater where it competes with arsenic for surface sites. Both arsenic and phosphate are tetrahedral oxyanions and have similar adsorption envelopes for oxide minerals with substantial adsorption occurring across a wide pH range (24). As(V) and PO_4^{3-} sorb as inner-sphere complexes via ligand exchange and have similar deprotonation constants (6). At a higher phosphate ratio, 1:10 As:PO_4^{3-}, Dixit and Hering found that arsenate adsorption decreases more

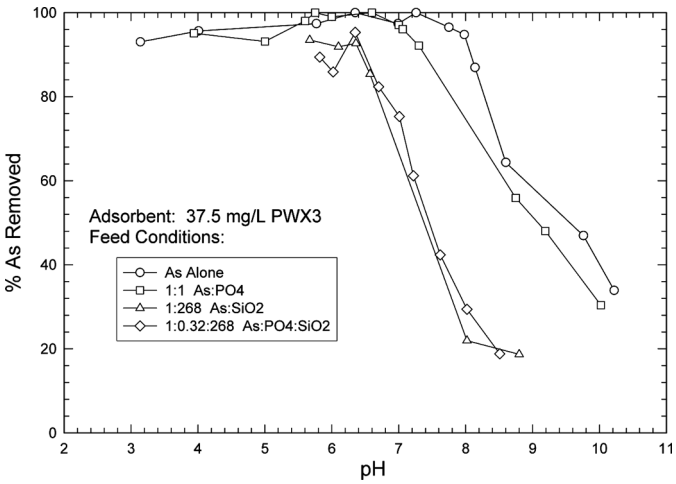

FIG. 9. pH adsorption edges for PWX3 removal of arsenic alone and with competition present. Adsorbent concentration of 37.5 mg/L and feed conditions shown.

dramatically from 100% to 60% at a pH of 4 for iron oxide, with similar results for goethite (25). Viloante and Pigna, working with goethite and gibbsite, also reported decreased As(V) sorption with increased initial PO_4^{3-}:As(V) molar ratios (27). Although it is still unclear as to the actual bonding mechanism on the surface, Manning and Goldberg have proposed that the goethite surface contains adsorption sites that are capable of sorbing either As(V) or PO_4^{3-} anions, and sites that adsorb either one or the other (24). In addition, Hongshao and Stanforth analyzed competitive adsorption to better understand the bonding mechanisms for arsenate and phosphate on goethite (28). Their results indicate a two-phase surface reaction that begins with a rapid surface complex formation followed by a slower build up of surface precipitate on the adsorbed layer. The exchangeable anions are in the surface precipitate and competition between co-occurring adsorbates may be influenced by kinetics of adsorption reactions (10).

It is apparent that the similarity in structure and adsorption envelopes of phosphate with As(V) results in a decrease in removal of As(V) with increased PO_4^{3-} concentration with either anion being sorbed by adsorption sites and adsorption kinetics impacting the exchange in the surface precipitate.

SiO_2, at a 1:268 As:SiO_2 molar ratio, reduced the amount of arsenic adsorbed by 40% to 64% between pH 6.4 and 8.8. The effect of PO_4^{3-} and SiO_2 together was nearly the same as SiO_2 alone, most likely as a result of the higher concentration of SiO_2. Working with bauxol, Gene and Tjell found that when the molar ratios are similar, PO_4^{3-} has a greater effect than SiO_2 (17) again most likely due to the similarity in structure and adsorption envelope of phosphate and As(V). Studying the desorption of arsenic from AA and GFH, Ghosh et al. found that PO_4^{3-} replaced arsenic from sorbent surface sites at a much higher level than silicate on a per mole basis (29).

Soluble silica exhibits high affinity for surfaces of aluminum and ferric oxides (6). Working with ferrihydrite, Singh et al. proposed that the silicate effect is due to a combination of complexation reactions between Fe(III), Si(IV), and As(V) species and competition between As(V) and Si(IV) for adsorption sites (30). Another factor identified by Wilkie and Hering, was that competition between co-curring adsorbates may be influenced by kinetics of the adsorption reactions (10).

Adsorption Isotherms

Adsorption data were modeled using the Langmuir and Freundlich isotherms. For the Langmuir isotherm, adsorption is limited by surface saturation and reaches a maximum density (10):

$$q = \frac{q_{\max} C_e}{K_d + C_e} \tag{1}$$

q = mass of adsorbate adsorbed per unit mass of adsorbent, mg adsorbate/g adsorbent.

q_{max} = maximum capacity, mg adsorbate/g adsorbent.

C_e = adsorbate equilibrium aqueous phase concentration, μg/L.

$K_d = 1/K_{ads}$ the partition coefficient (slope of the linear portion of the isotherm at high mass/low contaminant levels), L/mg.

$$K_{ads} = \frac{[S - As(V)]}{[S][As(V)]} \tag{2}$$

[S] = concentration of available surface sites.

[As(V)] = concentration of As(V) in solution.

[S − As(V)] = concentration of adsorbate bound to surface sites.

Where the absorption of As(V) onto the adsorbent is a reversible reaction with a limited, monolayer adsorption capacity.

$$S + As(V) \Leftrightarrow S - As(V) \tag{3}$$

The Freundlich isotherm, an empirical relationship is written as:

$$q = K_f C_e^{1/n} \tag{4}$$

K_f = Freundlich capacity factor, $L^{1/n}$ $\mu g^{1-1/n}$/mg

1/n = Freundlich intensity parameter

Freundlich and Langmuir isotherms were generated for PWX5 and E-33 as-received material and by particle size. With an initial arsenic concentration of 100 μg/L, both the Freundlich and Langmuir models generated high R^2 values (generally between 0.95 and 0.99 as shown in Table 3 along with model parameters); however, the best fit for both PWX5 and E-33 was the Langmuir model. The Langmuir results, shown in Figs. 10–12, indicate a high correlation between the data and the model. As there are a finite number of surface sites on the adsorbent and the Langmuir model predicts As(V) removal by specific sites with a finite capacity—compared to the Freundlich which predicts unlimited capacity—only the Langmuir isotherm predictions are presented.

For an initial As(V) concentration of 100 μg/L (see Figs. 10 and 11), PWX5 q_{max} values ranged from 5.4 to 7.5 μg As/mg PWX5 with no correlation to particle size. For the predominant sizes (18×30 and 30×40) and the as-received material, the range was much narrower (6.8 to 7.5 μg As/mg PWX5). E-33 q_{max} values were higher, ranging from 7.56 to 12.86 μg As/mg E-33 with the as-received E-33

TABLE 3
Langmuir and Freundlich isotherm parameters and R^2 values

Langmuir Parameters				Freundlich Parameters			
Size	R^2	q_{max} (mg/g)	K_d (L/mg)	Size	R^2	K_f ($L^{1/n}\mu g^{1-1/n}$/mg)	1/n
			E-33				
16 × 18	0.933	7.561	2.674	16 × 18	0.901	2.83	0.24
18 × 30	0.953	12.861	8.763				
30 × 40	0.933	11.746	4.614	30 × 40	0.926	3.69	0.28
40 × 60	0.952	9.158	4.998	40 × 60	0.959	2.61	0.32
As received	0.948	9.539	4.165				
			PWX5 100 ppb				
16 × 18	0.986	5.589	2.434	16 × 18	0.965	2.53	0.20
18 × 30	0.868	6.752	1.875	18 × 30	0.927	3.32	0.18
30 × 40	0.950	7.474	2.766	30 × 40	0.977	2.37	0.29
40 × 60	0.949	5.365	0.872	40 × 60	0.872	3.36	0.12
As received	0.946	7.306	2.601	As received	0.971	2.72	0.26
			PWX5 500 ppb				
16 × 18	0.907	7.81	5.45				
18 × 30	0.895	7.87	3.62				
30 × 40	0.973	9.68	9.41				
40 × 60	0.962	8.01	10.17				
As received	0.978	10.89	8.12				

q_{max} equal to 9.5 μg As/mg E-33. These results fall in the range of 3.7 to 13 μg As/mg spent GFH reported by Driehaus et al. for Berlin tap water, with an average arsenic content of 8.4 μg As/mg GFH (5). The E-33 isotherm results did not show a correlation to particle size. These results appear to be inconsistent with those of Yean et al., who determined that arsenic adsorption maximum capacity was a function of particle size for magnetite with arsenic having a greater affinity for the smaller particles. However, when the surface area was factored in, Yean et al. determined the maximum capacities for the different particle sizes were similar (20). In addition, the E-33 particles physically degraded during the shaking period, increasing, the surface area and accessibility to the iron, likely resulting in artificially high q_{max} values.

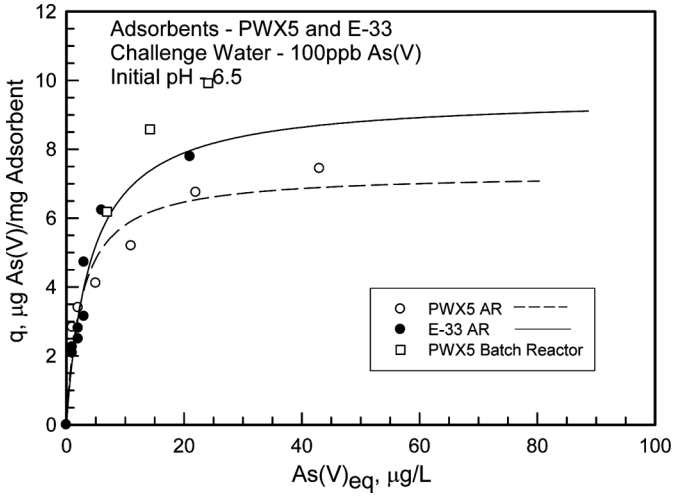

FIG. 10. Isotherm comparing adsorption of As(V) by PWX5 and E-33 for as-received (AR) particle size.

Langmuir isotherms were also developed for PWX5 with an initial arsenic concentration of 500 ppb, shown in Fig. 12. The resultant q_{max} values were higher than those generated for 100 ppb, ranging from 7.8 to 10.9 μg As/mg PWX5. The increased adsorption is due to the greater driving force of the arsenic in solution which resulted in bonding with weaker surface sites. In addition, q_{max} was higher as a result of lower As:SiO_2 and As:PO_4^{3-} molar ratios. Wilkie and Hering accounted for the effect of total As(III) concentration on adsorption by introducing surface heterogeneity. The effect on As(V) appeared to be similar but due to the high level of adsorption, the results were less conclusive (10).

Adsorption capacity and rate have been known to be affected by the temperature at which the adsorption process is conducted. Isotherms developed for PWX5 at 1°C, 22°C, and 36°C and presented in Fig. 13, show that q_{max} increases with increasing temperature (1°C–6.72; 22°C–7.31; and 36°C–9.01), but the K_d values do not correlate with temperature (1°C–4.32; 22°C–2.60; and 36°C–8.225). The increase in q_{max} may be a result of the existence of multiple types of sites with different activation energies. However, the K_d - rate of adsorption results are not consistent with

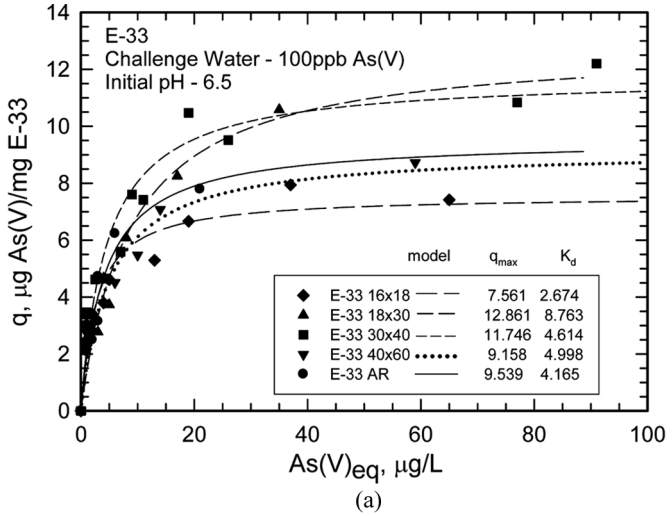

(a)

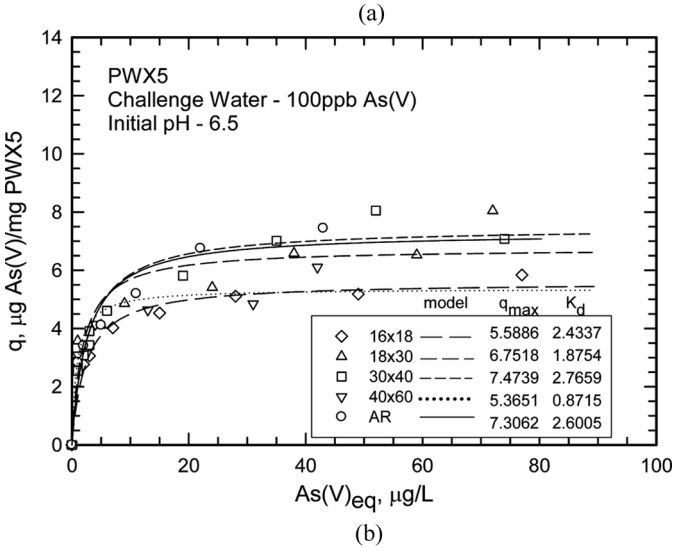

(b)

FIG. 11. Isotherms comparing adsorption of As(V) by particle size for a. E-33 b. PWX5.

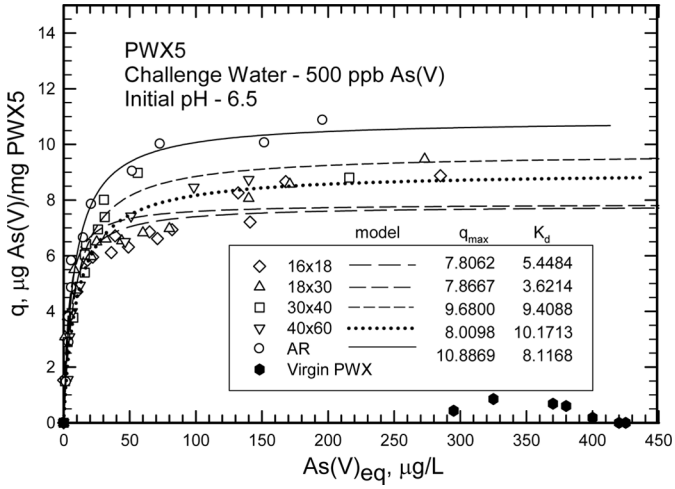

FIG. 12. Isotherm comparing adsorption of As(V) by PWX5 by particle size with a challenge Water As(V) concentration of 500 ppb.

work done by Banerjee et al. that demonstrated the adsorption of As(V) and As(III) by GFH was a spontaneous endothermic process at the temperatures tested with the overall adsorption reaction rate constant values increasing with increasing temperature (31).

When comparing the mass of arsenic adsorbed in relation to the mass of iron in the adsorbent, the q_{max} for as-received PWX5 was found to be about three times higher than the q_{max} for E-33: 45.7 µg As/mg Fe (34.0 mmol As/mol Fe) for PWX5 compared to 15.1 µg As/mg Fe (11.3 mmol As/mol Fe) for E-33. Dixit and Hering found a similar maximum sorption density of 16 mmol As/mol Fe for goethite (25). These results reinforce the conclusion that the E-33 removal sites are not as accessible or there are fewer sites compared with PWX5. Prior results for GFH and other iron containing adsorbents range from as little as 0.441 to 55.85 mmol As/mol Fe under similar conditions to as high as 600 mmol As/mol Fe at maximum adsorption for hydrous ferric oxide (HFO) (5,7,20,25, 32–35). A higher molar ratio of arsenic removed to iron indicates that PWX5 has a higher efficiency for arsenic removal due to the accessibility of the sites.

Removal Kinetics

The transport of arsenic ions from the bulk aqueous phase to internal adsorption sites consists of four steps: transport through the bulk liquid to the stagnant layer, film diffusion, pore diffusion, and chemical bonding at the particle surface. Film diffusion and pore diffusion mass transfer processes are considered the rate limiting steps (36,37). The rate of uptake is therefore a function of the adsorbent pore structure (size and tortuosity) and the hydrodynamics at the liquid/solid interface. The solutions were vigorously stirred throughout the experiment to minimize film resistance and

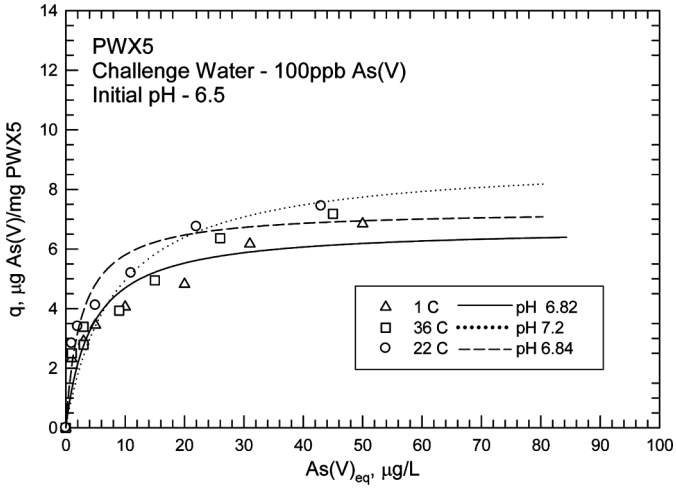

FIG. 13. Isotherm comparing adsorption of arsenic by PWX5 by temperature.

ensure intraparticle diffusion provided the driving force and governed the overall rate. The vortex in each beaker was maintained at the same depth for consistency in solution velocity, although some slight variations were observed in the movement of the particles (the larger particles did not disperse as high or as quickly as the smaller particles). Because the solution velocity is the same, the stagnant film layer thickness for the particles should be comparable.

The results of the stirred-batch reactor tests were modeled using a three parameter exponential decay model with:

$$C(t) = C_e + a \cdot e^{-kt} \quad (5)$$

where, C(t) is the arsenic concentration in the bulk phase at time "t" in μg/L; C_e is the equilibrium arsenic concentration in μg/L; "a" is a fitting parameter; and "k" is the adsorption rate in hr^{-1}.

The exponential decay model results, presented in Fig. 14, show that a correlation exists between the rate of arsenic adsorption and PWX5 particle size - the value of k increased with decreasing particle size. Since the hydrodynamic conditions were essentially the same, the adsorption rate variation is due to the adsorbent's size—for smaller particles the pore length is shorter and the adsorption rate faster. Although the rate of adsorption increased with decreasing particle size, there was little difference in the total amount of arsenic adsorbed indicating that iron oxide site accessibility was similar for different sized particles. The pH of the solution was largely maintained between 6.5 and 6.7, as shown in Fig. 14 to minimize the effects of pH on adsorption.

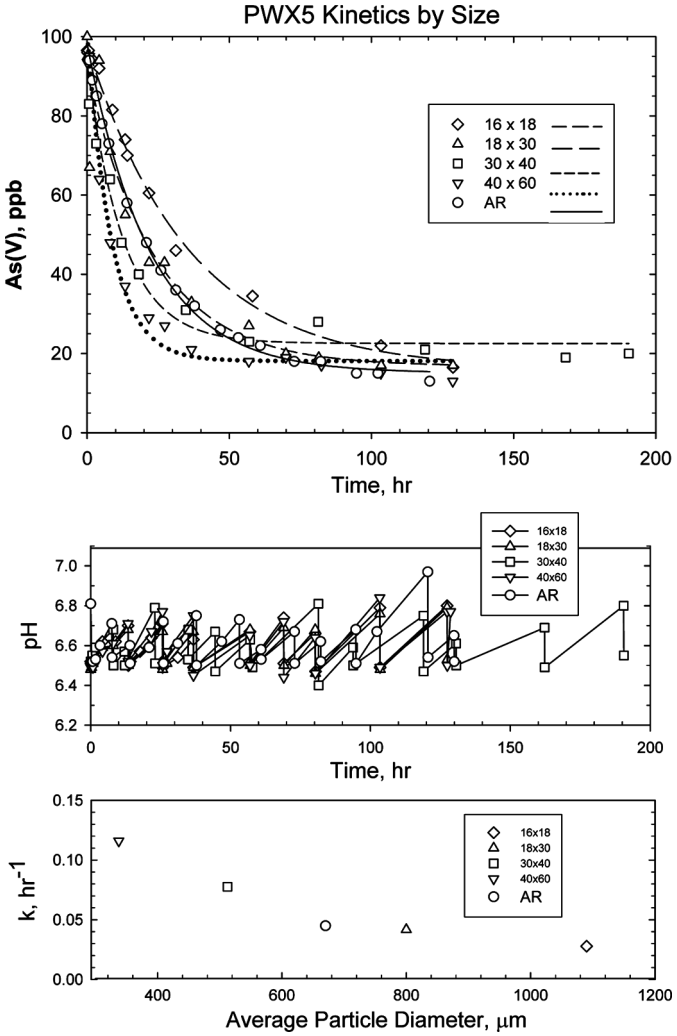

FIG. 14. Stirred-batch reactor results for 20 mg/L PWX5, modeled using exponential decay with three parameters comparing arsenic removal as a function of particle size. Adsorption rate comparison and pH drift/adjustment are also depicted.

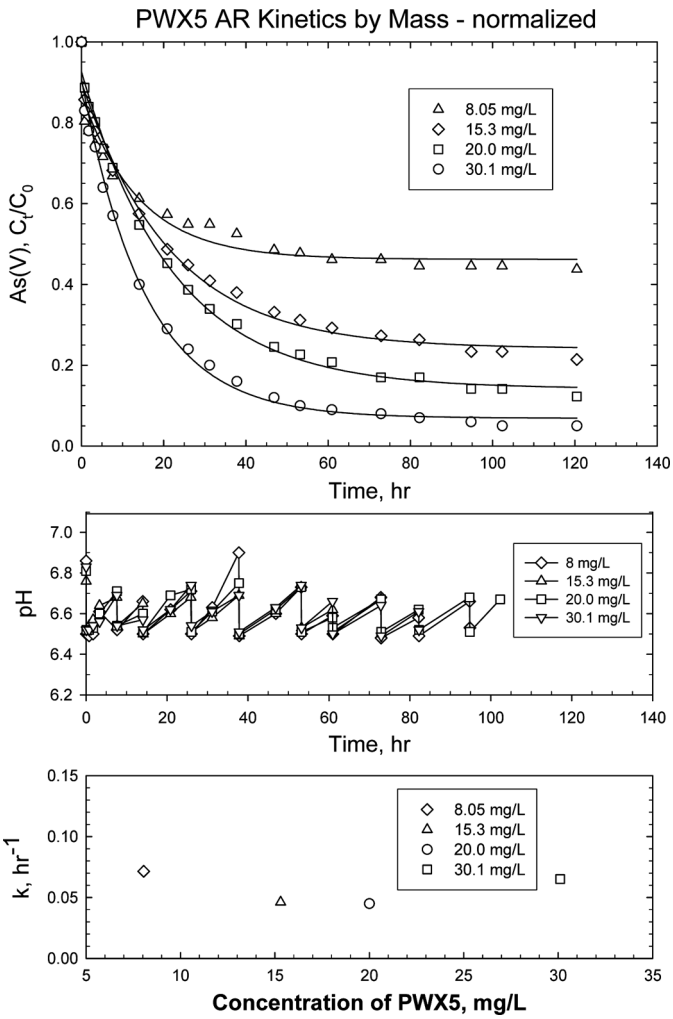

FIG. 15. Stirred-batch reactor results for PWX5 as-received particle size modeled using exponential decay with three parameters comparing arsenic removal as a function of mass. Adsorption rate comparison and pH drift/adjustment are also depicted.

TABLE 4
Stirred-batch reactor equilibrium concentration (C_e) and adsorption rates (k) for PWX5 by particle size (at 20 mg/L) and by concentration

	Ce (μg/L)	k (hr^{-1})	R^2
PWX5 Particle size			
40 × 60	18.1	0.116	0.982
30 × 40	22.5	0.078	0.974
As Received	14.2	0.045	0.994
18 × 30	16.8	0.042	0.932
16 × 18	15.9	0.028	0.995
PWX5 Concentration			
8.05 mg/L	46.2	0.072	0.934
15.3 mg/L	24.1	0.046	0.986
20.0 mg/L	14.2	0.045	0.994
30.1 mg/L	6.9	0.065	0.992

In Fig. 15, kinetic data are presented as a function of PWX5 concentration. As expected, the amount of arsenic adsorbed increased with increasing concentration of PWX5 due to the availability of additional adsorption sites; however, the rate of adsorption was fairly consistent for concentrations between 8.05 and 30.1 mg/L. The adsorption rates ranged between 0.045 and 0.0715 hr^{-1}, which are within the rates calculated for 20 mg/L solutions of the predominant particle sizes: 0.0418 hr^{-1} for 18 × 30 and 0.0777 hr^{-1} for 30 × 40. R^2 values for the model ranged from 0.932 to 0.995. The findings, presented in Table 4, differed with the expectations of the authors that the k values would increase with increasing concentration due to the presence of more sites near the particle external surface which results in a shorter travel distance.

Arsenic removal was rapid during the first 24 hours then slowed significantly as the equilibrium concentration was approached, which is typical of most adsorbents. Initially, As(V) rapidly formed bonds with strong surface adsorption sites. Over the next two days, the rate of adsorption progressively slowed as the concentration of As(V) in solution decreased. During this period, the As(V) formed bonds with the weaker available surface adsorption sites and diffused into the pores until equilibrium was reached.

CONCLUSION

As(V) removal is a function of pH, As(V) concentration, temperature, competition, adsorbent concentration, iron content, and iron accessibility. Although the capacity of PWX5 for As(V) removal is not a function of particle size, removal kinetics are. PWX5 and E-33 are effective at removing As(V) from drinking water, but the use of PWX5 is potentially more conducive for plant operations because of its durability and its homogeneous size. Although E-33 contains almost four times as much iron as PWX5, the PWX5 removed three times as many moles of As(V) per mole of iron. It is hypothesized that the PWX5 adsorption sites are either much more accessible, more numerous, or have stronger binding energies than the commercial grade E-33 that was studied. Generating isotherm data using ground E-33 overestimates As(V) removal capacity which will lead to an over estimation of the life of fixed bed systems.

PWX5 and E-33 remove As(V) by adsorption via ligand exchange with highest removal occurring below pH 7.0. At higher adsorbent concentrations, the adsorption edge moves to the right. Although higher adsorbent concentrations result in an overall increase in As(V) removal, the amount of arsenic removed per mole of iron decreases as the driving force for the As(V) in solution to exchange with weaker sites diminishes. Removal is also dependent on the presence of phosphate and silicate which reduce the amount of As(V) adsorbed, with silicate having the greatest impact as a result of the high SiO_2 concentration of the challenge water.

PWX5 adsorption of As(V) is limited by surface saturation and reaches a maximum density. Although independent of particle size, q_{max} increases as the initial arsenic concentration increases and as temperature increases. The rate of adsorption is dependent on particle size, increasing with a decreasing diameter due to shorter pore length, but it is not a function of adsorbent concentration.

Although results from batch testing cannot be directly transferred to fixed bed columns due to differences in kinetics conditions, it is apparent that PWX5 is effective at removing arsenic with iron content and accessibility, particle size, temperature, competition, and pH factoring into the amount and rate of As(V) adsorbed by the material, and it is a viable alternative to other iron-based adsorbents for adsorption systems used to meet the new 10 μg/L maximum contaminant level.

ACKNOWLEDGEMENTS

This work was conducted in part with financial and technical support provided by Rohm and Haas Company.

REFERENCES

1. Smedley, P.L.; Kinniburgh, D.G. (2002) A review of the source, behaviour and distribution of arsenic in natural water. *Applied Geochemistry*, 17 (5): 517–568.
2. The Council of the European Union. (1998) Council directive 98/83/EC of 3 November 1998 on the quality of water intended for human consumption. *Official Journal of the European Communities 5.12.98*, 330: 32–54.
3. US Environmental Protection Agency. (2001) National primary drinking water regulations; arsenic and clarifications to compliance and new source contaminants monitoring. *Federal Register: January 22, 2001*, 66 (l4): 6975–7066.

4. Manju, G.N.; Raji, C.; Anirudhan, T.S. (1998) Evaluation of cocpnut husk carbon for the removal of arsenic from water. *Water Research*, 32 (10): 3062–3070.
5. Driehaus, W.; Jekel, M.; Hildebrandt, U. (1998) Granular ferric hydroxide - a new adsorbent for the removal of arsenic from natural water. *Journal of Water SRT -Aqua (Oxford)*, 47 (1): 30–35.
6. Mohapatra, D.; Singh, P.; Zhang, W.; Pullammanappallil, P. (2005) The effect of citrate, oxalate, acetate, silicate and phosphate on stability of synthetic arsenic-loaded ferrihydrite and Al-ferrihydrite. *Journal of Hazardous Materials*, 124 (1–3): 95–100.
7. Saha, B.; Bains, R.; Greenwood, F. (2005) Physicochemical characterization of granular ferric hydorxide (GFH) for arsenic(V) sorption from water. *Separation Science and Technology*, 40: 2909–2932.
8. Rosengrant, L.; Fargo, L. (1990) Final best demonstrated available technology (BDAT) background document for K031, K084, K101, K102, As wastes (D004), Se wastes (DO 10), and P and U wastes containing arsenic and selenium listing constituents. In: *Report EPA/530/SW-90/059A*, U.S. EPA, vol. 1, pp. 1–124.
9. Ghosh, M.M.; Teoh, R.S. (1985) Adsorption of arsenic on hydrous aluminum oxides. *Proceedings of Mid-Atlantic Industrial Waste Conference*, pp. 139–155.
10. Wilkie, J.A.; Hering, J.G. (1996) Adsorption of arsenic onto hydrous ferric oxide: effects of adsorbate/adsorbent ratios and co-occurring solutes. *Colloids and Surfaces A: Physicochemical and Engineering Aspects*, 107: 97–110.
11. Selvin, N.; Messham, G.; Simms, J.; Pearson, I.; Hall, J. (2000) The development of granular ferric media – arsenic removal and additional uses in water treatment. *Proceedings – Water Quality Technology Conference*, Salt Lake City: UT, pp. 483–494.
12. Amy, G.; Edwards, M.; Brandhuber, P.; McNeill, L.; Benjamin, M.; Vagliasindi, F.; Carlson, K.; Chwirka, J. (2000) *Arsenic Treatability Options and Evaluation of Residuals Management Issues*; American Water Works Association: CO.
13. Siegel, M.; Aragon, A.; Zhao, H.; Deng, S.; Nocon, M.; Aragon, M. (2008) Prediction of arsenic removal by adsorptive media: Comparison of field and laboratory studies. In: *Arsenic Contamination of Groundwater*, John Wiley & Sons, Inc.: North Carolina, Chapter 10, 227–268.
14. Westerhoff, P.; Haan, M.; Martindale, A.; Badruzzaman, M. (2006) Arsenic adsorptive media technology selection strategies. *Water Quality Research Journal of Canada*, 41 (2): 171–184.
15. An, B.; Steinwinder, T.; Zhao, D. (2005) Selective removal of arsenate from drinking water using a polymeric ligand exchanger. *Water Research*, 39 (20): 4993–5004.
16. Hering, J.G.; Chen, P.; Wilkie, J.A.; Elimelech, M.; Liang, S. (1996) Arsenic removal by ferric chloride. *Journal/American Water Works Association*, 88 (4): 155–167.
17. Genc, H.; Tjell, J.C. (2003) Effects of phosphate, silicate, sulphate, and bicarbonate on arsenate removal using activated seawater neutralised red mud (bauxsol). *Journal De Physique. IV: JP*, 107 (1): 537–540.
18. O'Connor, J.T. (2002) Arsenic in drinking water. Part 3: Occurence of arsenic in U.S. waters. *Water Engineering and Management*, 149 (5): 45–48.
19. Aragon, M.; Everett, R.; Siegel, M.; Kottenstette, R.; Holub, W.; Wright, J.; Dwyer, B. (2007) Arsenic pilot plant operation and results – Socorro Springs, New Mexico – phase 1. In: *Sandia National Laboratories Technical Report*, SAND2007–3255: NM and CA, 1–34.
20. Yean, S.; Cong, L.; Yavuz, C.T.; Mayo, J.T.; Yu, W.W.; Kan, A.T.; Colvin, V.L.; Tomson, M.B. (2005) Effect of magnetite particle size on adsorption and desorption of arsenite and arsenate. *Journal of Materials Research*, 20 (12): 3255–3264.
21. vanLoon, G.W.; Duffy, S.J. (2005) *Environmental Chemistry A Global Perspective*, 2nd Ed.; Oxford University Press: UK.
22. Lin, T.F.; Liu, C.C.; Hsieh, W.H. (2006) Adsorption kinetics and equilibrium of arsenic onto an iron-based adsorbent and an ion exchange resin. *Water Science and Technology: Water Supply*, 6 (2): 201–207.
23. Vaughan, R.L.; Reed, B.E. (2005) Modeling As(V) removal by a iron oxide impregnated activated carbon using the surface complexation approach. *Water Research*, 39 (6): 1005–1014.
24. Manning, B.A.; Goldberg, S. (1996) Modeling competitive adsorption of arsenate with phosphate and molybdate on oxide minerals. *Soil Science Society of America Journal*, 60 (1): 121–131.
25. Dixit, S.; Hering, J.G. (2003) Comparison of arsenic(V) and arsenic(III) sorption onto iron oxide minerals: Implications for arsenic mobility. *Environmental Science and Technology*, 37 (18): 4182–4189.
26. Edwards, M.; Patel, S.; McNeill, L.; Chen, H.; Frey, M.; Eaton, A.D.; Antweiler, R.C.; Taylor, H.E. (1998) Considerations in As analysis and speciation. *Journal/American Water Works Association*, 90 (3): 103–113.
27. Violante, A.; Pigna, M. (2002) Competitive sorption of arsenate and phosphate on different clay minerals and soils. *Soil Science Society of America Journal*, 66: 1788.
28. Hongshao, Z.; Stanforth, R. (2001) Competitive adsorption of phosphate and arsenate on goethite. *Environmental Science and Technology*, 35 (24): 4753–4757.
29. Ghosh, A.; Sáez, A.E.; Ela, W. (2006) Effect of pH, competitive anions and NOM on the leaching of arsenic from solid residuals. *Science of the Total Environment*, 363 (1–3): 46–59.
30. Singh, P.; Zhang, W.; Muir, D.M.; Robins, R.G. (2005) The effect of silicate on the adsorption of arsenate on coprecipitated ferrihydrite. In: *Arsenic Metallurgy - Proceedings of the Symposium held during The Minerals, Metals and Materials Society, TMS 2005 Annual Meeting*, pp. 129–135.
31. Banerjee, K.; Amyb, G.L.; Prevostc, M.; Nourc, S.; Jekeld, M.; Gallaghera, P.M.; Blumenscheine, C.D. (2008) Kinetic and thermodynamic aspects of adsorption of arsenic onto granular ferric hydroxide (GFH). *Water Research*, 42 (13): 3371–3378.
32. Reed, B.E.; Vaughan, R.; Jiang, L. (2000) As(III), As(V), Hg, and Pb removal by Fe- oxide impregnated activated carbon. *Journal of Environmental Engineering*, 126 (9): 869–873.
33. Thirunavukkarasu, O.S.; Viraraghavan, T.; Subramanian, K.S. (2003) Arsenic removal from drinking water using granular ferric hydroxide. *Water SA*, 29 (2): 161–170.
34. Raven, K.P.; Jain, A.; Loeppert, R.H. (1998) Arsenite and arsenate adsorption on ferrihydrite: Kinetics, equilibrium, and adsorption envelopes. *Environmental Science and Technology*, 32: 344–349.
35. Fuller, C.C.; Davis, J.A.; Waychunas, G.A. (1993) Surface chemistry of ferrihydrite: Part 2. Kinetics of arsenate adsorption and coprecipitation. *Geochimica et Cosmochimica Acta*, 57 (10): 2271–2282.
36. Lin, T.-F.; Wu, J-K. (2001) Adsorption of arsenite and arsenate within activated alumina grains: Equilibrium and kinetics. *Water Research*, 35 (8): 2049–2057.
37. Chen, W.; Parette, R.; Zou, J.; Cannon, F.S.; Dempsey, B.A. (2007) Arsenic removal by iron-modified activated carbon. *Water Research*, 41: 1851–1858.